Supplementary Information

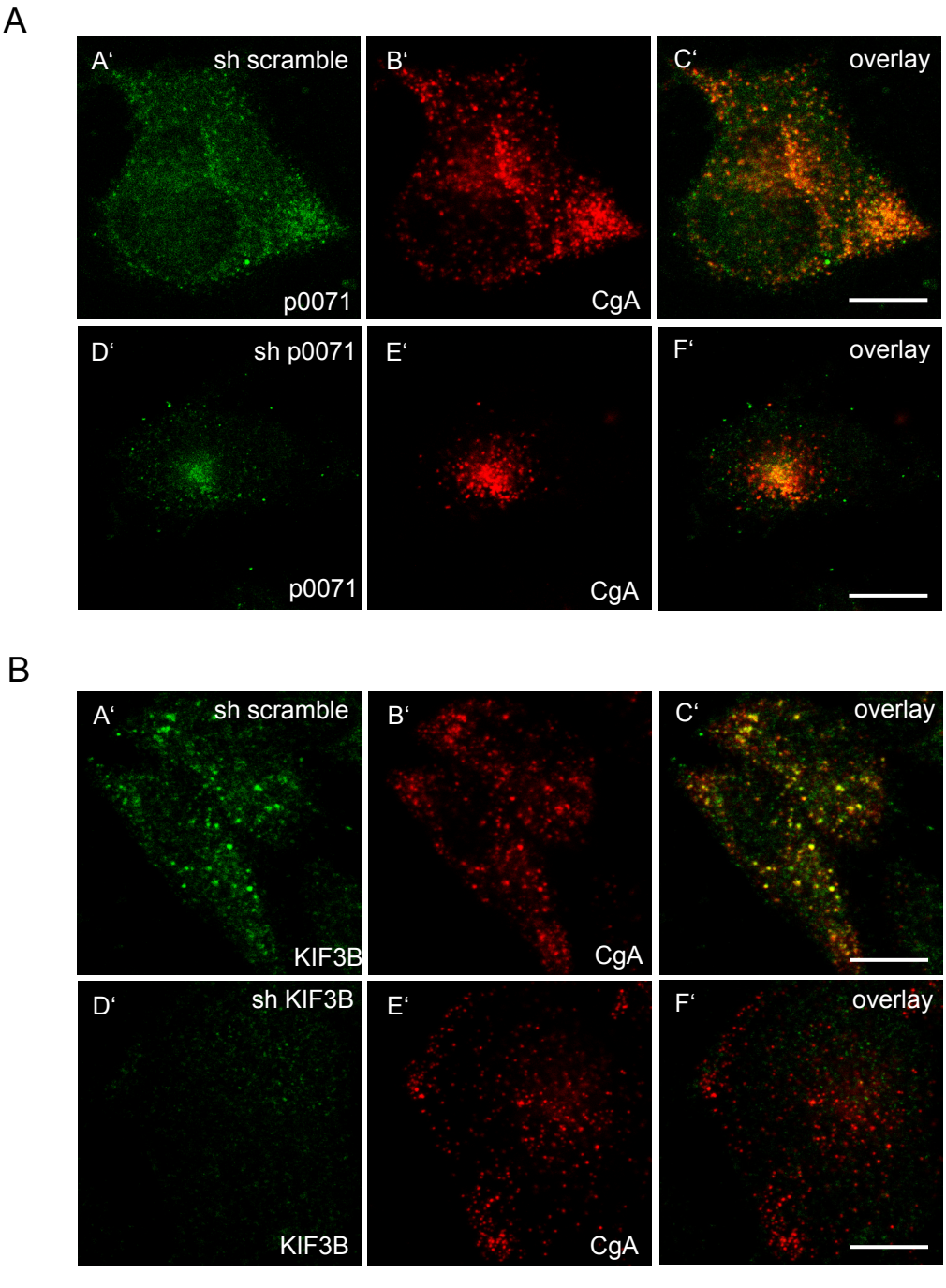

Fig. S1. Specificity of antibodies used in immunofluorescence staining. (A) Confocal image sections of BON cells treated with control or p0071- targeted shRNA, fixed and stained with antibodies against p0071 and chromogranin A. The specific localization of p0071 as described in Fig. 1B is lost upon p0071 depletion despite a weak residual staining in the perinuclear area. Scale bar: 10μm (B) Confocal image sections of BON cells stained for KIF3B and CgA. Signal intensity and specific co-localization of KIF3B with CgA-positive vesicles is lost upon knockdown of KIF3B. Scale bar: 10μm.

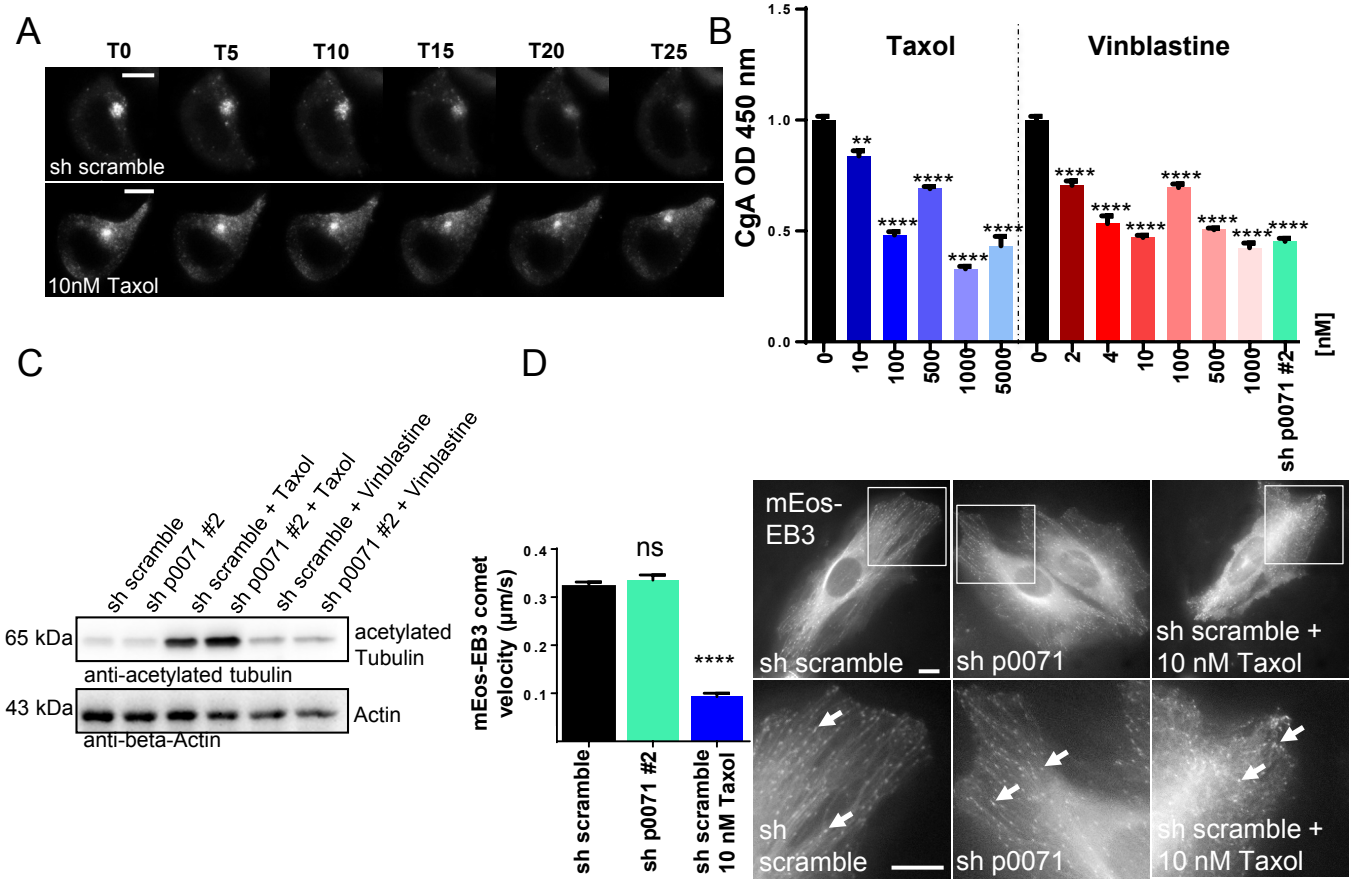

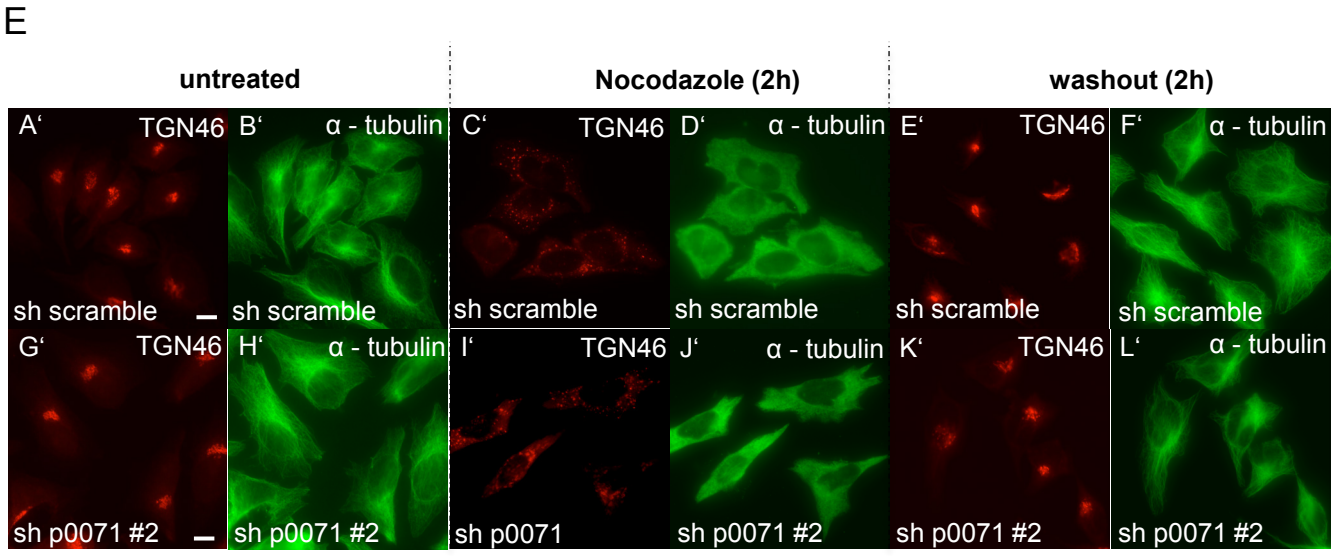

Fig. S2. P0071 depletion does not affect microtubule network and Golgi organization. (A) CgA-GFP time-lapse microscopy in BON cells. Images have been extracted from a live cell video series showing intracellular fluorescence intensity of CgA-GFP after temperature-mediated block at the TGN and subsequent re-initiation of secretion over a time period of 25 minutes. Incubation of BON cells with 10nM taxol impaired CgA release indicated by enhanced intracellular CgA-GFP fluorescence after 25 minutes. The control cell with scrambled shRNA (upper panel) is also depicted in Fig. 2A as part of an experiment performed together with the taxol treatment. Scale bars: 7.5µm. (B) Treatment of BON cells with microtubule targeting agents taxol and vinblastine impairs CgA secretion. BON cells were incubated over night with the indicated doses of drugs, and effects were compared to p0071 knockdown. Mean and SEM from n=6 experiments. $^{**}P<0.01$, $^{****}P<0.0001$ (two-tailed unpaired Student's *t*-test). (C) Knockdown of p0071 in HeLa cells does not change alpha-tubulin acetylation, in contrast to taxol (10nM) or vinblastine (5nM), as shown by western blot and an acetylation specific antibody. (D) End-binding protein mEOS-EB3 tracking microcopy. mEOS-EB3 was transiently expressed in HeLa cells to monitor microtubule plus-end polymerization. Cells treated with p0071 shRNA were compared to control cells and cells incubated with taxol (10nM) over night (see images in right panel). Fifty particles per condition were tracked over 5 seconds and velocities were quantified (left panel). The graph represents mean and SEM, $^{****}P<0.0001$ (two-tailed unpaired Student's *t*-test). (E) Nocodazole washout experiments in HeLa cells. HeLa cells (treated with control shRNA and shp0071, respectively) were exposed to nocodazole for 2 hours before intensive washout. Cells were fixed and stained for alpha-tubulin (green) and the TGN marker TGN46 (red) before treatment, after incubation with nocodazole and at 2 hours following washout. Golgi disruption and microtubule organization after nocodazole treatment and after re-organization following washout is shown for all samples.

Figure S3

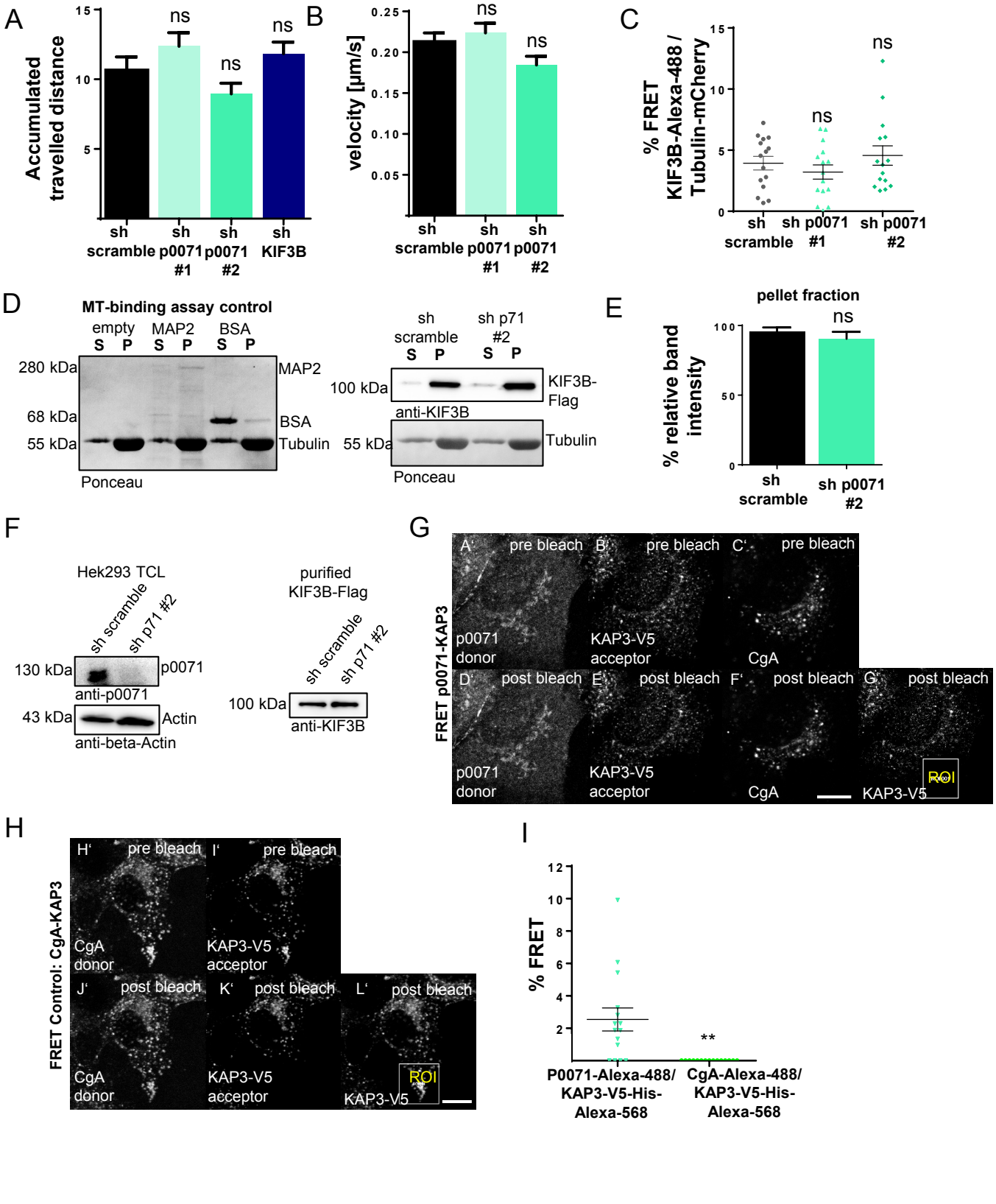

Fig. S3. Molecular interactions of KIF3 complex proteins. (A) Accumulated distance (accounting for movement in both directions from the tracking starting point) of CgA-GFP vesicles in BON cells traced in live cell imaging videos quantified in Fig. 5 A-C. Forty tracks per condition (control shRNA; shp0071 # 1&2; shKif3B) were observed and quantified for as long as they were present in the focus layer. (B) Velocities of vesicles in BON cells treated with control shRNA and shp0071, respectively, were quantified as described in A). Velocities are shown in µm per second. (C) Binding of the KIF3B motor proteins to microtubules. Quantitative AB-FRET analysis of KIF3B labeled by Alexa-488 dye and transiently expressed alpha-tubulin-mCherry in BON cells treated with scrambled shRNA or two different shRNAs directed against p0071, respectively. The graph shows the mean and SEM %FRET (*n*=15 cells and three independent experiments). ns, not significant (two-tailed unpaired Student's *t*-test). (D) Left-hand side: Microtubule binding spin-down assay control experiment showing specific interaction of the microtubule associated protein MAP2A and BSA as negative control. Right-hand side: Microtubule binding assay performed with KIF3B-Flag protein purified from control cells and cells depleted of p0071, respectively. (E) Statistical analysis of KIF3B-Flag amount detected in pellet fractions relative to total amount of KIF3B-Flag used in assays (pellet + sup). Integrated band intensities from n=3 experiments; ns, no significant differences in KIF3 complex binding to microtubules. (F) Left-hand side: Verification of p0071 knockdown in Hek293 cells used for KIF3B-Flag expression and purification. Right-hand side: Western blot of KIF3B-Flag protein used for microtubule binding studies shown in D) and E). (G) Interaction of endogenous p0071 labeled by anti-p0071 and Alexa-488 antibodies (donor; A'; D') with KAP3-V5-His probed by anti-V5 and Alexa-568 secondary antibodies (acceptor; B'; E'). Interaction was quantified by AB-FRET in the cytosolic region of BON cells containing CgA granula stained by anti-CgA and Alexa-647 antibodies (C'; F'). The bleach-region (ROI) is shown in (G'). Scale bar: 10 µm (H) The cargo CgA contained in vesicles labeled by anti-CgA and Alexa-488 antibodies was used a non-interacting negative control for FRET experiments together with KAP3-V5-His stained by anti-V5 and Alexa-568 antibodies (H' to K', the bleach- ROI is shown in (L'). Scale bar: 10 µm. (I) Statistical analysis of 15 cells from G and H. Mean and SEM %FRET; ns, non significant (two-tailed unpaired Student's *t*-test).

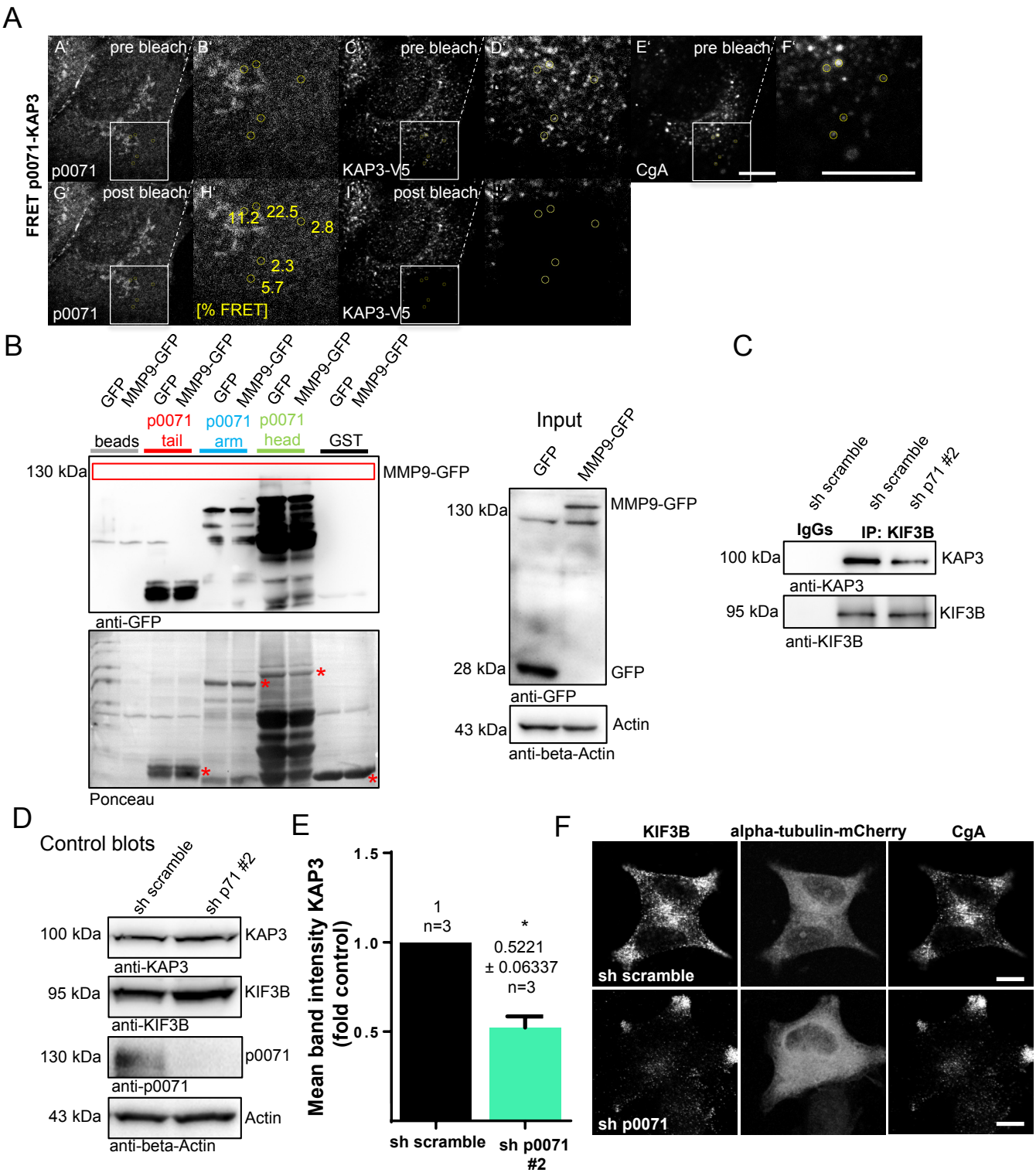

Fig. S4. KAP3 and p0071 binding studies. (A) Representative Sub-ROI analysis for the interaction of p0071 (A'; G'; magnifications B' and H', respectively) and KAP3-V5-His (C'; I'; magnifications D' and J', respectively) at vesicular structures marked by CgA staining (E'; F') in BON cells. Sub-ROIs are highlighted by yellow circles around CgA-positive structures (E'; F'). %FRET of individual Sub-ROIs is shown as yellow numbers in H'. Scale bar: 10 µm. (B) Left-hand panel: Control pulldown experiments to demonstrate lack of binding of MMP-9 to individual domains of p0071. MMP-9-GFP was expressed in HEK293T cells and cell lysates were incubated with purified GST-p0071-head, GST-p0071-armadillo repeat and GST-p0071 tail domains immobilized on GST-sepharose beads, respectively. Empty beads and GST-loaded beads as well as HEK293T lysates transfected with empty vector were used as negative controls. Ponceau staining of the respective membrane shows the presence of GST proteins. Asterisks mark the full-length GST proteins. Right-hand panel: Expression of KAP3-V5-His in HEK293T cells. (C) Co-immunoprecipitation experiments were performed as described in Fig. 7A using a second p0071-directed shRNA (shp0071 #2). KAP3 signals were normalized to the intensities of KIF3B IP bands. (D) Control blots showing protein expression in total cell lysates from cells used in C). (E) Statistical analysis of co-precipitated KAP3 in KIF3B IPs. N=3 experiments, mean and SEM, **P*<0.05 (two-tailed paired Student's *t*-test). (F) Representative images of BON cells used for KIF3B signal intensity analysis as shown in Fig. 7E, F. Cells were treated with scrambled shRNA and p0071-directed shRNA (shp0071 #1), respectively and transfected to express alpha-tubulin-mCherry . KIF3B and CgA were stained with specific primary and secondary antibodies.

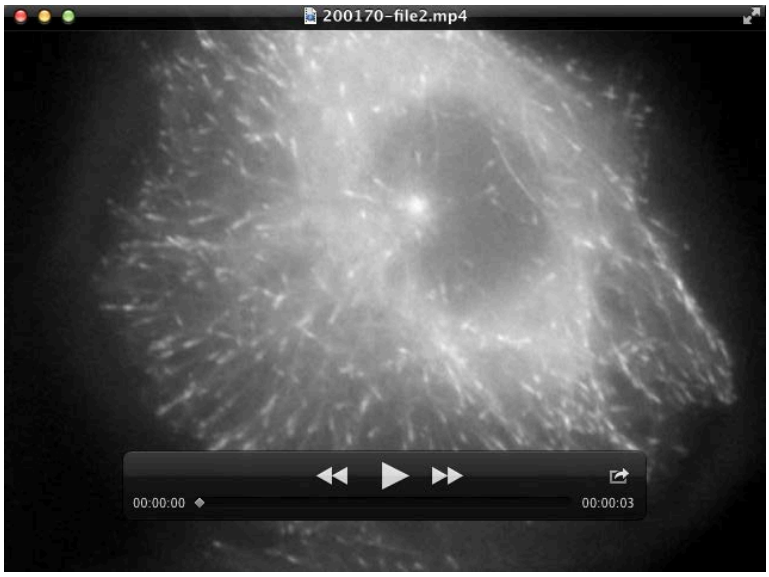

Movie S1. mEos-EB3 comet tracking in a HeLa cell. HeLa cells treated with scrambled shRNA were transfected to express mEos-EB3. End-point tracking was performed at 37°C using an inverted Olympus IX71 microscope (Olympus, Hamburg, Germany) and quantified with the ImageJ manual tracking tool (Schindelin et al., 2015).

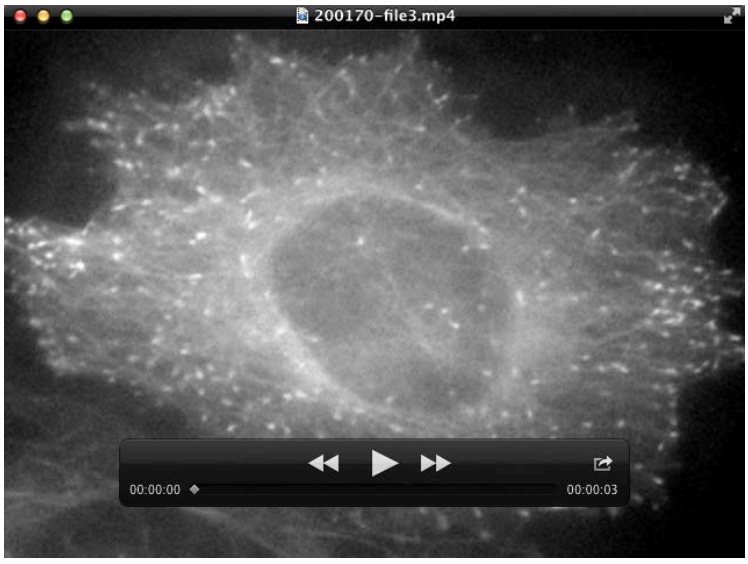

Movie S2. mEos-EB3 comet tracking in a p0071-knockdown HeLa cell. P0071 was knocked down in HeLa cells using a specific shRNA and cells were transfected to express mEos-EB3. End-point tracking was performed at 37°C using an inverted Olympus IX71 microscope (Olympus, Hamburg, Germany) and quantified with the ImageJ manual tracking tool (Schindelin et al., 2015).

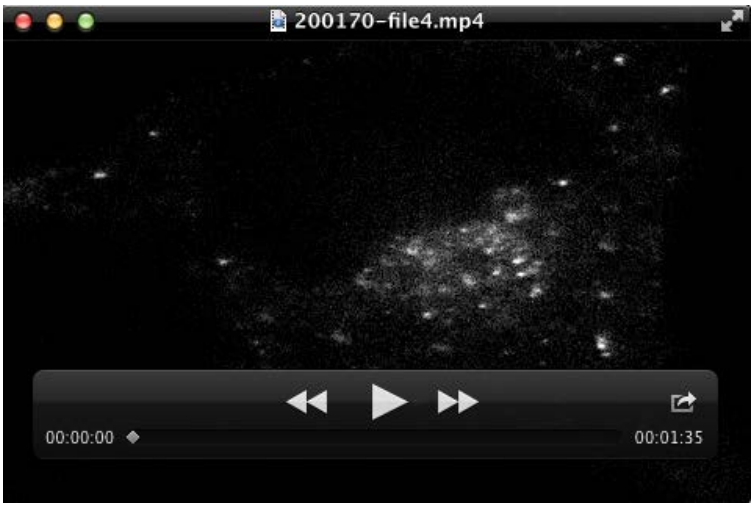

Movie S3. Movement of CgA vesicles in a BON cell. Cells were treated with scrambled shRNA and transfected to transiently express CgA-GFP. Cargo retention was induced at 18°C and re-release initiated at permissive temperature. Live imaging was carried out at 37°C using a confocal laser-scanning microscope and vesicles (seen as bright rounded structures) were tracked in several cells within the cytoplasmic area using the ImageJ manual Tracking tool (Schindelin et al., 2015).

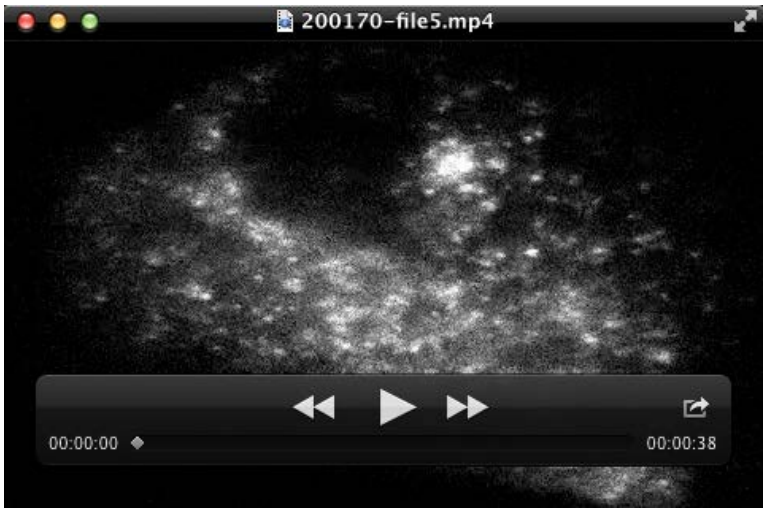

Movie S4. Erratical movement of CgA vesicles in a p0071 depleted BON cell. Cells were treated with p0071-directed shRNA and transfected to transiently express CgA-GFP. Cargo retention was induced at 18°C and re-release initiated at permissive temperature. Live imaging was carried out at 37°C using a confocal laser-scanning microscope and intracellularly accumulated CgA vesicles were tracked in several cells within the cytoplasmic area using the ImageJ manual Tracking tool (Schindelin et al., 2015).

Table S1: List of primary and secondary antibodies with ordering number, company name, dilution and references of usage. WB: Western blot, IF: Immunofluorescence, IP: Immunoprecipitation.

Name	ordering number	company	Dilution	References
p0071	GP71	Progen, Heidelberg, Germany	IF: 1:50 IP: 2µg	(Hofmann et al., 2008; Hofmann et al., 2009; Medvetz et al., 2012)
KIF3B	sc-50456	St Cruz, Santa Cruz, CA, USA	IF: 1:100 WB: 1:1000 IP: 2µg	(Aguado-Fraile et al., 2012; Keil et al., 2009)
KAP3	sc-55598	St Cruz, Santa Cruz, CA, USA	IF: 1:100 WB: 1:1000	(Landers et al., 2009; Traynor et al., 2010)
alpha-tubulin	T5168	Sigma Aldrich, St Louis, MO, USA	IF: 1:200 WB: 1:1000	(Lefave et al., 2011; Whelan et al., 2010)
TGN46	NBP1-49643	Novus Biologicals, Littleton, CO, USA	IF: 1:500	(Eiseler et al., 2016; Wille et al., 2014)
chromogranin A	M086929-2	DAKO, St Clara, CA, USA	IF: 1:100	(Aguilera et al., 2015; Gradiz et al., 2016; Scharfmann et al., 2014)
beta-actin	#A2228	Sigma Aldrich, St Louis, MO, USA	WB: 1:2000	(Darr et al., 2014; Wohlfert et al., 2006; Zhao et al., 2011)
Flag-M2	#F1804	Sigma Aldrich, St Louis, MO, USA	WB: 1:2000 IP: 2µg	(Han et al., 2010; He et al., 2010; Kinsey et al., 2009; Rudinskiy et al., 2009)
p0071	651166	Progen, Heidelberg, Germany	WB: 1:100	(Hofmann et al., 2008; Hofmann et al., 2009)
PKD2	A300-073A	Bethyl, Montgomery, TX, USA	WB: 1:1000	(Azoitei et al., 2011; Irie et al., 2012; Zheng et al., 2011)
acetylated tubulin	ab125356	Abcam, Cambridge, UK	WB: 1:1000	(Mori et al., 2015; Smirnova et al., 2016; Xiaojun et al., 2016)
V5 epitope	ab3792	Millipore, Billerica, MA, USA	WB: 1:2000	(Cui et al., 2015; Jablonski et al., 2015; Minoura et al., 2016)
Anti-guinea pig FITC	F-7762	Sigma Aldrich, St Louis, MO, USA	IF: 1:400	(Geffrotin et al., 2000; Kasimiotis et al., 2000; Makarenko et al., 2002)
Alexa-Fluor 568/647 goat-anti-rabbit	# A11036 # A21244	Thermo Scientific, Carlsbad, CA, USA	IF: 1:400	(Eiseler et al., 2010; Eiseler et al., 2012; Eiseler et al., 2015; Wille et al., 2014)
Alexa-Fluor 488/568 goat-anti-mouse	#A11029 #A11031	Thermo Scientific, Carlsbad, CA, USA	IF: 1:400	(Eiseler et al., 2010; Eiseler et al., 2012; Eiseler et al., 2015; Wille et al., 2014)
Alexa-Fluor 488 goat-anti-guinea pig	#A11073	Thermo Scientific, Carlsbad, CA, USA	IF: 1:400	(Baer et al., 2012; Checchi et al., 2014; Housley et al., 2013)

References

Aguado-Fraile, E., Ramos, E., Saenz-Morales, D., Conde, E., Blanco-Sanchez, I., Stamatakis, K., del Peso, L., Cuppen, E., Brune, B. and Bermejo, M. L. (2012). miR-127 protects proximal tubule cells against ischemia/reperfusion: identification of kinesin family member 3B as miR-127 target. *PLoS One* **7**, e44305.

Aguilera, O., Gonzalez-Sancho, J. M., Zazo, S., Rincon, R., Fernandez, A. F., Tapia, O., Canals, F., Morte, B., Calvanese, V., Orgaz, J. L. et al. (2015). Nuclear DICKKOPF-1 as a biomarker of chemoresistance and poor clinical outcome in colorectal cancer. *Oncotarget* **6**, 5903-17.

Azoitei, N., Kleger, A., Schoo, N., Thal, D. R., Brunner, C., Pusapati, G. V., Filatova, A., Genze, F., Moller, P., Acker, T. et al. (2011). Protein kinase D2 is a novel regulator of glioblastoma growth and tumor formation. *Neuro Oncol* **13**, 710-24.

Baer, M. M., Palm, W., Eaton, S., Leptin, M. and Affolter, M. (2012). Microsomal triacylglycerol transfer protein (MTP) is required to expand tracheal lumen in Drosophila in a cell-autonomous manner. *J Cell Sci* **125**, 6038-48.

Checchi, P. M., Lawrence, K. S., Van, M. V., Larson, B. J. and Engebrecht, J. (2014). Pseudosynapsis and decreased stringency of meiotic repair pathway choice on the hemizygous sex chromosome of Caenorhabditis elegans males. *Genetics* **197**, 543-60.

Cui, J., Xiao, J., Tagliabracci, V. S., Wen, J., Rahdar, M. and Dixon, J. E. (2015). A secretory kinase complex regulates extracellular protein phosphorylation. *Elife* **4**, e06120.

Darr, J., Klochendler, A., Isaac, S. and Eden, A. (2014). Loss of IGFBP7 expression and persistent AKT activation contribute to SMARCB1/Snf5-mediated tumorigenesis. *Oncogene* **33**, 3024-32.

Eiseler, T., Hausser, A., De Kimpe, L., Van Lint, J. and Pfizenmaier, K. (2010). Protein kinase D controls actin polymerization and cell motility through phosphorylation of cortactin. *J Biol Chem* **285**, 18672-83.

Eiseler, T., Kohler, C., Nimmagadda, S. C., Jamali, A., Funk, N., Joodi, G., Storz, P. and Seufferlein, T. (2012). Protein kinase D1 mediates anchorage-dependent and -independent growth of tumor cells via the zinc finger transcription factor Snail1. *J Biol Chem* **287**, 32367-80.

Eiseler, T., Wille, C., Koehler, C., Illing, A. and Seufferlein, T. (2015). Protein kinase D2 assembles a multiprotein complex at the Trans-Golgi-network to regulate matrix metalloproteinase secretion. *J Biol Chem*.

Eiseler, T., Wille, C., Koehler, C., Illing, A. and Seufferlein, T. (2016). Protein Kinase D2 Assembles a Multiprotein Complex at the Trans-Golgi Network to Regulate Matrix Metalloproteinase Secretion. *J Biol Chem* **291**, 462-77.

Geffrotin, C., Horak, V., Crechet, F., Tricaud, Y., Lethias, C., Vincent-Naulleau, S. and Vielh, P. (2000). Opposite regulation of tenascin-C and tenascin-X in MeLiM swine heritable cutaneous malignant melanoma. *Biochim Biophys Acta* **1524**, 196-202.

Gradiz, R., Silva, H. C., Carvalho, L., Botelho, M. F. and Mota-Pinto, A. (2016). MIA PaCa-2 and PANC-1 - pancreas ductal adenocarcinoma cell lines with neuroendocrine differentiation and somatostatin receptors. *Sci Rep* **6**, 21648.

Han, Y., Huang, C., Sun, X., Xiang, B., Wang, M., Yeh, E. T., Chen, Y., Li, H., Shi, G., Cang, H. et al. (2010). SENP3-mediated de-conjugation of SUMO2/3 from promyelocytic leukemia is correlated with accelerated cell proliferation under mild oxidative stress. *J Biol Chem* **285**, 12906-15.

He, S., McPhaul, C., Li, J. Z., Garuti, R., Kinch, L., Grishin, N. V., Cohen, J. C. and Hobbs, H. H. (2010). A sequence variation (I148M) in PNPLA3 associated with nonalcoholic fatty liver disease disrupts triglyceride hydrolysis. *J Biol Chem* **285**, 6706-15.

Hofmann, I., Kuhn, C. and Franke, W. W. (2008). Protein p0071, a major plaque protein of non-desmosomal adhering junctions, is a selective cell-type marker. *Cell Tissue Res* **334**, 381-99.

Hofmann, I., Schlechter, T., Kuhn, C., Hergt, M. and Franke, W. W. (2009). Protein p0071 - an armadillo plaque protein that characterizes a specific subtype of adherens junctions. *J Cell Sci* **122**, 21-4.

Housley, G. D., Morton-Jones, R., Vlajkovic, S. M., Telang, R. S., Paramananthasivam, V., Tadros, S. F., Wong, A. C., Froud, K. E., Cederholm, J. M., Sivakumaran, Y. et al. (2013). ATP-gated ion channels mediate adaptation to elevated sound levels. *Proc Natl Acad Sci U S A* **110**, 7494-9.

Irie, A., Harada, K., Araki, N. and Nishimura, Y. (2012). Phosphorylation of SET protein at Ser171 by protein kinase D2 diminishes its inhibitory effect on protein phosphatase 2A. *PLoS One* **7**, e51242.

Jablonski, A. M., Lamitina, T., Liachko, N. F., Sabatella, M., Lu, J., Zhang, L., Ostrow, L. W., Gupta, P., Wu, C. Y., Doshi, S. et al. (2015). Loss of RAD-23 Protects Against Models of Motor Neuron Disease by Enhancing Mutant Protein Clearance. *J Neurosci* **35**, 14286-306.

Kasimiotis, H., Myers, M. A., Argentaro, A., Mertin, S., Fida, S., Ferraro, T., Olsson, J., Rowley, M. J. and Harley, V. R. (2000). Sex-determining region Y-related protein SOX13 is a diabetes autoantigen expressed in pancreatic islets. *Diabetes* **49**, 555-61.

Keil, R., Kiessling, C. and Hatzfeld, M. (2009). Targeting of p0071 to the midbody depends on KIF3. *J Cell Sci* **122**, 1174-83.

Kinsey, M., Smith, R., Iyer, A. K., McCabe, E. R. and Lessnick, S. L. (2009). EWS/FLI and its downstream target NR0B1 interact directly to modulate transcription and oncogenesis in Ewing's sarcoma. *Cancer Res* **69**, 9047-55.

Landers, J. E., Melki, J., Meininger, V., Glass, J. D., van den Berg, L. H., van Es, M. A., Sapp, P. C., van Vught, P. W., McKenna-Yasek, D. M., Blauw, H. M. et al. (2009). Reduced expression of the Kinesin-Associated Protein 3 (KIFAP3) gene increases survival in sporadic amyotrophic lateral sclerosis. *Proc Natl Acad Sci U S A* **106**, 9004-9.

Lefave, C. V., Squatrito, M., Vorlova, S., Rocco, G. L., Brennan, C. W., Holland, E. C., Pan, Y. X. and Cartegni, L. (2011). Splicing factor hnRNPH drives an oncogenic splicing switch in gliomas. *EMBO J* **30**, 4084-97.

Makarenko, I. G., Meguid, M. M. and Ugrumov, M. V. (2002). Distribution of serotonin 5-hydroxytriptamine 1B (5-HT(1B)) receptors in the normal rat hypothalamus. *Neurosci Lett* **328**, 155-9.

Medvetz, D. A., Khabibullin, D., Hariharan, V., Ongusaha, P. P., Goncharova, E. A., Schlechter, T., Darling, T. N., Hofmann, I., Krymskaya, V. P., Liao, J. K. et al. (2012). Folliculin, the product of the Birt-Hogg-Dube tumor suppressor gene, interacts with the adherens junction protein p0071 to regulate cell-cell adhesion. *PLoS One* **7**, e47842.

Minoura, I., Takazaki, H., Ayukawa, R., Saruta, C., Hachikubo, Y., Uchimura, S., Hida, T., Kamiguchi, H., Shimogori, T. and Muto, E. (2016). Reversal of axonal growth defects in an extraocular fibrosis model by engineering the kinesin-microtubule interface. *Nat Commun* **7**, 10058.

Mori, M., Mahoney, J. E., Stupnikov, M. R., Paez-Cortez, J. R., Szymaniak, A. D., Varelas, X., Herrick, D. B., Schwob, J., Zhang, H. and Cardoso, W. V. (2015). Notch3-Jagged signaling controls the pool of undifferentiated airway progenitors. *Development* **142**, 258-67.

Rudinskiy, N., Grishchuk, Y., Vaslin, A., Puyal, J., Delacourte, A., Hirling, H., Clarke, P. G. and Luthi-Carter, R. (2009). Calpain hydrolysis of alpha- and beta2-adaptins decreases clathrin-dependent endocytosis and may promote neurodegeneration. *J Biol Chem* **284**, 12447-58.

Scharfmann, R., Pechberty, S., Hazhouz, Y., von Bulow, M., Bricout-Neveu, E., Grenier-Godard, M., Guez, F., Rachdi, L., Lohmann, M., Czernichow, P. et al. (2014).

Development of a conditionally immortalized human pancreatic beta cell line. *J Clin Invest* **124**, 2087-98.

Smirnova, N. F., Schamberger, A. C., Nayakanti, S., Hatz, R., Behr, J. and Eickelberg, O. (2016). Detection and quantification of epithelial progenitor cell populations in human healthy and IPF lungs. *Respir Res* **17**, 83.

Traynor, B. J., Nalls, M., Lai, S. L., Gibbs, R. J., Schymick, J. C., Arepalli, S., Hernandez, D., van der Brug, M. P., Johnson, J. O., Dillman, A. et al. (2010). Kinesin-associated protein 3 (KIFAP3) has no effect on survival in a population-based cohort of ALS patients. *Proc Natl Acad Sci U S A* **107**, 12335-8.

Whelan, S. A., Dias, W. B., Thiruneelakantapillai, L., Lane, M. D. and Hart, G. W. (2010). Regulation of insulin receptor substrate 1 (IRS-1)/AKT kinase-mediated insulin signaling by O-Linked beta-N-acetylglucosamine in 3T3-L1 adipocytes. *J Biol Chem* **285**, 5204-11.

Wille, C., Kohler, C., Armacki, M., Jamali, A., Gossele, U., Pfizenmaier, K., Seufferlein, T. and Eiseler, T. (2014). Protein kinase D2 induces invasion of pancreatic cancer cells by regulating matrix metalloproteinases. *Mol Biol Cell* **25**, 324-36.

Wohlfert, E. A., Gorelik, L., Mittler, R., Flavell, R. A. and Clark, R. B. (2006). Cutting edge: deficiency in the E3 ubiquitin ligase Cbl-b results in a multifunctional defect in T cell TGF-beta sensitivity in vitro and in vivo. *J Immunol* **176**, 1316-20.

Xiaojun, W., Yan, L., Hong, X., Xianghong, Z., Shifeng, L., Dingjie, X., Xuemin, G., Lijuan, Z., Bonan, Z., Zhongqiu, W. et al. (2016). Acetylated alpha-Tubulin Regulated by N-Acetyl-Seryl-Aspartyl-Lysyl-Proline(Ac-SDKP) Exerts the Anti-fibrotic Effect in Rat Lung Fibrosis Induced by Silica. *Sci Rep* **6**, 32257.

Zhao, X., Kuja-Panula, J., Rouhiainen, A., Chen, Y. C., Panula, P. and Rauvala, H. (2011). High mobility group box-1 (HMGB1; amphoterin) is required for zebrafish brain development. *J Biol Chem* **286**, 23200-13.

Zheng, H., Qian, J., Varghese, B., Baker, D. P. and Fuchs, S. (2011). Ligand-stimulated downregulation of the alpha interferon receptor: role of protein kinase D2. *Mol Cell Biol* **31**, 710-20.